

Baryon fluctuation signatures of the onset of deconfinement

Marek Gazdzicki^a, Mark I. Gorenstein^b, Anar Rustamov^c

^a*Jan Kochanowski University, Kielce, Poland*

^b*Bogolyubov Institute for Theoretical Physics, Kyiv, Ukraine*

^c*GSI Helmholtzzentrum für Schwerionenforschung, Darmstadt, Germany*

Abstract

An anomalous collision-energy dependence of proton number fluctuations is predicted as a consequence of the onset of deconfinement in heavy-ion collisions at the center of mass energy of the nucleon pair $\sqrt{s_{NN}} \approx 10$ GeV. The effect arises from changes in the effective degrees of freedom between confined and deconfined matter. This may provide a natural explanation of the recent beam-energy-scan results on proton number fluctuations at the BNL RHIC and offers a consistent interpretation of data from the CERN SPS and RHIC experiments in terms of the onset of deconfinement.

Keywords: heavy-ion collisions, onset of deconfinement, fluctuations, baryons and protons

1. Introduction

The discovery of the high-density state of strongly interacting matter – the quark-gluon plasma (QGP) [1] – has been the primary goal of the experimental studies of high-energy nucleus-nucleus collisions. One of the key results was the observation of the rapid changes in hadron production properties in central Pb+Pb collisions at $\sqrt{s_{NN}} \approx 8$ GeV by the NA49 experiment [2, 3].

This collision energy was expected [4] for the onset of deconfinement – the beginning of the creation of a deconfined state of strongly interacting matter with increasing collision energy. These experimental results were confirmed by the RHIC beam energy program [5], and the LHC results support their interpretation (see Ref. [6] and references therein).

In parallel, the search for the conjectured critical point – the endpoint of the first order phase transitions in the QCD phase diagram – has been pursued at the CERN SPS and BNL RHIC; see Refs. [7, 8] for reviews. The collision energy dependence of proton number fluctuations has been measured over a broad range of energies by STAR [9, 10] at RHIC (BNL), HADES [11] at the SIS (GSI), and ALICE [12, 13] at the CERN LHC. The results indicate an anomalous energy dependence in central Au+Au collisions (see Ref. [14]). Hydrodynamics-based calculations of the experimental data on proton number fluctuations also suggest possible critical point effects at $\sqrt{s_{NN}} \leq 10$ GeV. More recently, it has been proposed that baryon–baryon interactions undergo a transition from predominantly repulsive to predominantly attractive at around $\sqrt{s_{NN}} \approx 10$ GeV [15]. In addition, modifications of baryon stopping across the onset of deconfinement were investigated in [16], where they were shown to have a significant impact on baryon number fluctuations.

In the present work, we predict the collision-energy dependence of fluctuations in the net-baryon and proton numbers near the onset of deconfinement. The ideal hadron resonance gas (HRG) and quark-gluon plasma (QGP) approaches are used to model confined and deconfined systems produced in heavy-ion collisions. First, the collision energy dependence of net-baryon number cumulants is calculated within the grand canonical ensemble.

ble (GCE). Then, predictions for limited momentum acceptance and global net-baryon conservation are obtained. Finally, we compute predictions for proton-number cumulants.

The paper is organised as follows. The basic idea is introduced in Sec. 2. The quantitative model is formulated, and its predictions are presented in Sec. 3. The discussion and conclusions close the paper in Sec. 4.

2. Intuitive arguments

It was suggested many years ago [17, 18] that the fluctuations of net baryon number and electric charge may be suppressed when deconfined matter is created. The idea explores the fact that, in confined matter, the units of baryon number and electric charge are unity, whereas in deconfined matter they are carried by quarks with fractional values: $1/3$ for baryon number and $1/3$ or $2/3$ for electric charge.

To illustrate the idea, we first discuss toy models of confined and deconfined matter, considering two systems within the GCE. The first system is filled with an ideal Boltzmann gas of baryons, while the second contains an ideal Boltzmann gas of quarks. Thus, the quark and baryon number distributions are Poissonian. Consequently, all cumulants ¹ coincide with the mean, and for the baryon gas all baryon number cumulant ratios are equal to unity.

¹In this paper, the first four cumulants are used. They are defined as: $\kappa_1[N] = E[N]$ (mean), $\kappa_2[N] = E[(N - E[N])^2]$ (variance), $\kappa_3[N] = E[(N - E[N])^3]$ (skewness numerator), $\kappa_4[N] = E[(N - E[N])^4] - 3E[(N - E[N])^2]^2$ (excess kurtosis numerator). The $E[N]$ stands for the expectation value of N .

Since baryons are formed from triplets of quarks, for sufficiently large number of quarks, the numbers of quarks and baryons are related by $N_b \approx N_q/3$. Consequently, the ratios of baryon number cumulants are

$$\frac{\kappa_2[N_b]}{\kappa_1[N_b]} \approx \frac{1}{3}, \quad \frac{\kappa_3[N_b]}{\kappa_2[N_b]} \approx \frac{1}{3}, \quad \frac{\kappa_4[N_b]}{\kappa_2[N_b]} \approx \frac{1}{9}. \quad (1)$$

Therefore, one expects that the energy dependence of cumulant ratios in heavy-ion collisions changes qualitatively during the transition from a confined to a deconfined system.

In addition to the fractional baryon charges of quarks, several important differences arise after deconfinement. First, the relevant degrees of freedom become light quarks whose masses are small compared with the system temperature, whereas the proton mass in the hadronic phase is much larger than the temperature. Second, a substantial population of antiquarks appears, while in the hadronic phase before the onset of deconfinement, the number of antibaryons is negligible. Third, Fermi–Dirac statistics plays an important role for the quark–antiquark system, whereas quantum-statistical effects are negligible for baryons. All these effects are quantified in the next section.

For completeness, we note that motivated by the ideas from Refs. [17, 18], net-electric charge fluctuations were measured and discussed in numerous studies. Here, we refer to the pioneering measurements by NA49 [19, 20] as well as more recent results from ALICE [21]. Significant uncertainties in modelling other processes that influence fluctuations have obscured conclusions regarding the observation of fractional electric charges [22]. It is even more challenging to observe fractional baryonic charges at the CERN LHC energies.

3. Baryon number fluctuations as the signal of the onset of deconfinement

We consider central heavy-ion collisions (Pb+Pb or Au+Au), neglecting, for simplicity, event-by-event fluctuations of the volume of the created system. We postulate that at the early stage of collisions at low energies ($\sqrt{s_{NN}} \leq 8$ GeV), the equilibrium HRG is created. In contrast, for energies $\sqrt{s_{NN}} \geq 12$ GeV [4, 23], the equilibrium QGP is formed.

Experiments measure the collision-energy dependence of fluctuations of proton and net-proton numbers. The latter is defined as the difference between proton and antiproton numbers. The results are obtained within a limited momentum acceptance. To calculate the corresponding predictions for the onset of deconfinement, we proceed in three steps. First, we calculate predictions for net-baryon number fluctuations in the GCE. Second, we account for the effect of global net-baryon conservation in a limited momentum acceptance. Third, we estimate the collision-energy dependence of proton-number cumulant ratios.

The GCE predictions for net-baryon fluctuations at collision energies $4 \leq \sqrt{s_{NN}} \leq 8$ GeV are calculated using the ideal-gas classical HRG². Fermi statistics and excluded-volume repulsion lead to only weak modifications of the results. We therefore assume Poisson distributions for the baryon and antibaryon numbers, N_b and $N_{\bar{b}}$. This leads to a Skellam distribution for the net-baryon number, $B = N_b - N_{\bar{b}}$.

²At $\sqrt{s_{NN}} \leq 4$ GeV, one expects the perceptible contribution to the baryon number fluctuations from nucleon clusters.

At $\sqrt{s_{NN}} \leq 8$ GeV, the antibaryon-to-baryon ratio is below 1% [24]. Therefore, the Skellam distribution of the net-baryon number is close to the Poisson distribution of baryons, which leads to

$$\frac{\kappa_2[B]_H}{\kappa_1[B]_H} = 1, \quad \frac{\kappa_3[B]_H}{\kappa_2[B]_H} = 1, \quad \frac{\kappa_4[B]_H}{\kappa_3[B]_H} = 1, \quad (2)$$

for the net-baryon-number cumulants ratios at $\sqrt{s_{NN}} \leq 8$ GeV. The subscript H denotes ratios calculated within the HRG model. The ratios are shown in Figs. 1 - 3 for collision energies from 4 to 8 GeV.

The net-baryon number fluctuations for the deconfined matter are calculated using the ideal-gas QGP equation of state with massless u , d , and s quarks. Within this model, the GCE pressure P as a function of temperature T and quark chemical potentials μ_f reads [25]

$$\frac{P}{T^4} = \sum_{f=u,d,s} \left[\frac{7\pi^2}{60} + \frac{1}{2} \left(\frac{\mu_f}{T} \right)^2 + \frac{1}{4\pi^2} \left(\frac{\mu_f}{T} \right)^4 \right], \quad (3)$$

where the chemical potentials of u , d , and s quarks are related to baryon and strangeness chemical potentials μ_B and μ_S as

$$\mu_u = \frac{1}{3}\mu_B, \quad \mu_d = \frac{1}{3}\mu_B, \quad \mu_s = \frac{1}{3}\mu_B - \mu_S = 0. \quad (4)$$

The factor 1/3 in Eq.(4) corresponds to the baryon number of quark. We take $\mu_S = \mu_B/3$ to ensure zero net-strangeness, and neglect the small values of μ_Q (for heavy-ion collisions, a rough estimate is $\mu_Q \approx -\mu_B/30$ [26]). The cumulants $\kappa_n[B]$ of the net-baryon number distribution follow from derivatives of the pressure with respect to the baryon chemical potential

$$\kappa_n[B]_Q = VT^3 \frac{\partial^n}{\partial (\mu_B/T)^n} \left(\frac{P}{T^4} \right), \quad n = 1, 2, 3, 4, \dots \quad (5)$$

This yields

$$\kappa_1[B]_Q = VT^3 \left[\frac{2}{9} \frac{\mu_B}{T} + \frac{2}{81\pi^2} \left(\frac{\mu_B}{T} \right)^3 \right], \quad (6)$$

$$\kappa_2[B]_Q = VT^3 \left[\frac{2}{9} + \frac{2}{27} \left(\frac{\mu_B}{\pi T} \right)^2 + \frac{1}{9} \right], \quad (7)$$

$$\kappa_3[B]_Q = VT^3 \left(\frac{4}{27\pi^2} \frac{\mu_B}{T} \right), \quad (8)$$

$$\kappa_4[B]_Q = VT^3 \left(\frac{4}{27\pi^2} + \frac{2}{27\pi^2} \right). \quad (9)$$

The subscript $_Q$ denotes cumulants calculated for the QGP. Note that strange quarks do not contribute to the odd cumulants since $\mu_s = 0$. However, they do contribute to the even cumulants. The last terms in the right-hand side of Eqs. (7) and (9) arise from strange–antistrange quark fluctuations at $\mu_s = 0$.

The corresponding cumulant ratios are

$$\frac{\kappa_2[B]_Q}{\kappa_1[B]_Q} = \frac{3}{2\pi z} \frac{9 + 2z^2}{9 + z^2}, \quad (10)$$

$$\frac{\kappa_3[B]_Q}{\kappa_2[B]_Q} = \frac{4z}{\pi(9 + 2z^2)}, \quad (11)$$

$$\frac{\kappa_4[B]_Q}{\kappa_2[B]_Q} = \frac{6}{\pi^2(9 + 2z^2)}, \quad (12)$$

where $z \equiv \mu_B/(\pi T)$. Note that the ratio $\kappa_2[B]/\kappa_1[B]$ diverges as $\mu_B \rightarrow 0$. Thus, this ratio is ill-defined when the net-baryon density vanishes, as in the case of collisions at the LHC.

The collision energy dependence of the net-baryon number cumulant ratios for QGP, calculated according to Eqs. (10) - (12), are shown in Figs. 1 - 3 for collision energies from 12 to 20 GeV. We assume that the QGP created at the early stage of the collision hadronizes close to the chemical freeze-out line. The cumulant predictions are then obtained using the energy-dependent

parametrization of T and μ_B : $T = a_1 - a_2\mu_B^2 - a_3\mu_B^4$ and $\mu_B = \frac{b_1}{1+b_2\sqrt{s_{NN}}}$, with $a_1 = 0.152$ GeV, $a_2 = 0.026$ GeV $^{-1}$, $a_3 = 0.219$ GeV $^{-3}$ and $b_1 = 1.310$ GeV, $b_2 = 0.278$ GeV $^{-1}$. The parametrisation was obtained by fitting the mean hadron multiplicities produced in central Pb+Pb and Au+Au collisions; see Ref. [27].

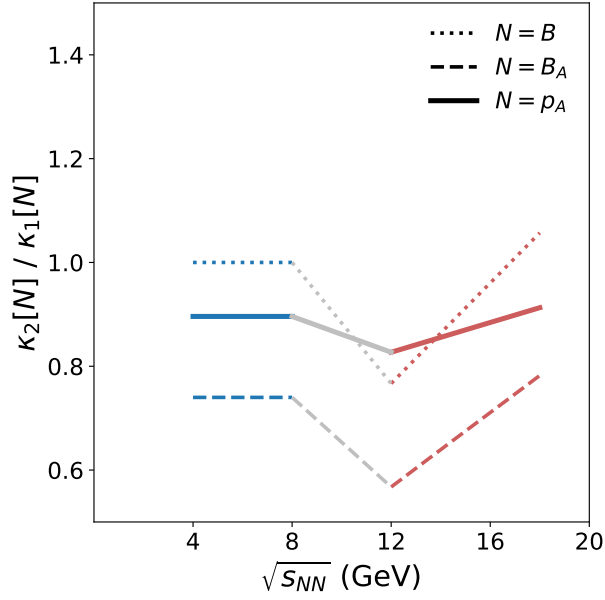


Figure 1: Collision energy dependence of the $\kappa_2[N]/\kappa_1[N]$ ratio predicted in the vicinity of the onset of deconfinement in heavy-ion collisions. Cumulants are calculated for the net baryon number within GCE ($N = B$), the net-baryon number within momentum acceptance taking into account net-baryon number conservation ($N = B_A$), and the proton number within the momentum acceptance ($N = p_A$). The lines indicated by light gray colour connect the HRG and QGP dependences across the changeover region to guide the eye.

In each collision, the total net-baryon number is conserved. However, the net-baryon number varies from collision to collision, if it is measured in a

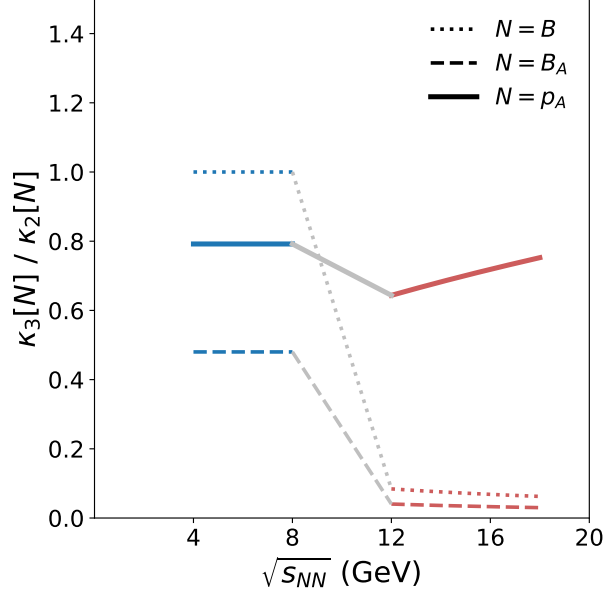


Figure 2: The same as in Fig. 1 but for $\kappa_3[N]/\kappa_2[N]$

limited momentum acceptance. Within the statistical approach, the effect of net-baryon number conservation in the limited-acceptance region can be modelled using the sub-ensemble acceptance method (SAM) introduced in Ref. [28]. It relates the GCE predictions to the corresponding expectations for a limited acceptance. For the considered cumulant ratios, one obtains

$$\frac{\kappa_2[B_A]}{\kappa_1[B_A]} = (1 - \alpha) \frac{\kappa_2[B]}{\kappa_1[B]}, \quad (13)$$

$$\frac{\kappa_3[B_A]}{\kappa_2[B_A]} = (1 - 2\alpha) \frac{\kappa_3[B]}{\kappa_2[B]}, \quad (14)$$

$$\frac{\kappa_4[B_A]}{\kappa_2[B_A]} = [1 - 3\alpha(1 - \alpha)] \frac{\kappa_4[B]}{\kappa_2[B]} - 3\alpha(1 - \alpha) \left(\frac{\kappa_3[B]}{\kappa_2[B]} \right)^2, \quad (15)$$

where B_A is the net-baryon number in the momentum acceptance and α

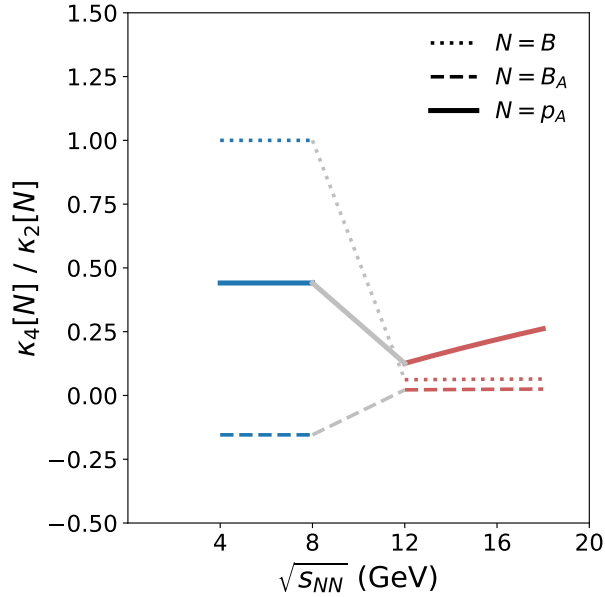


Figure 3: The same as in Fig. 1 but for $\kappa_4[N]/\kappa_2[N]$.

is the fraction of baryons in this acceptance. The relations were derived considering a limited acceptance in configuration space [28]. Obviously, the SAM method is also valid for particle selection in momentum space for models with uncorrelated particle production in both configuration and momentum spaces. In a more general situation, the applicability of the SAM method depends on the presence of a correlation between coordinate and momentum space, for example, due to the collective flow of matter; see Ref. [29] for details. In the absence of an alternative method, we employ the SAM method to estimate the predictions.

Figures 1 - 3 show predictions for the B_A cumulant ratios obtained using Eqs. (13) - (15). These equations are applied to the previously calculated

predictions for B cumulants obtained within GCE, i.e. Eq. (2) for the HRG and Eqs. (10) - (12) for the QGP. Here, a typical experimental value of the parameter $\alpha = 0.26$ was used [15].

The experiments measure fluctuations of proton number rather than of baryon number. To relate previously calculated net-baryon-number cumulant ratios in the acceptance to proton-number ratios, a hadronization model is required. At the considered collision energies ($\sqrt{s_{NN}} \lesssim 20$ GeV) the mean number of anti-baryons is smaller than 10% of the mean number of baryons [24]. Thus, we approximate the net-baryon-number cumulants by the baryon-number cumulants. Furthermore, we assume that for a fixed net-baryon number B_A , the proton number p_A fluctuates according to a binomial distribution with the probability β – the so-called binomial thinning. Under the binomial thinning, the cumulants are modified according to the standard relations given in Appendix A.

Figures 1 - 3 show predictions for the proton number cumulants calculated for the HRG and the QGP using Eqs. (A.1) - (A.3), applied to the previously calculated prediction for B_A cumulants, Eqs. (13) - (15). Here, a typical value of the parameter $\beta = 0.4$ was used [24].

4. Discussion and conclusions

The collision energy dependence of the net-baryon number in the GCE (B), net-baryon number in the momentum acceptance (B_A) and proton number in momentum acceptance (p_A) is predicted to change rapidly in the vicinity of the onset of deconfinement ($\sqrt{s_{NN}} \approx 8 - 12$ GeV). This is demonstrated in Figs. 1 - 3. The largest changes are observed for B and the smallest for

p_A . The magnitude of the change in the proton number cumulants ratios significantly depends on the fraction of accepted baryons (α) and the fraction of protons among the accepted baryons (β). In Appendix Appendix B, we present the collision-energy dependence of the proton-number factorial cumulant ratios measured in the STAR experiment together with the predictions obtained in this paper for the onset of deconfinement. The model calculations are done for parameters $\alpha = 0.26$ and $\beta = 0.4$, the typical experimental values for STAR [30, 9]. Both the data and the model exhibit a qualitative change in the collision-energy dependence at $\sqrt{s_{NN}} \approx 8\text{--}12$ GeV.

A quantitative comparison of the onset of deconfinement predictions with the experimental results requires, in particular,

- (i) using experimentally estimated values of the parameter α , which significantly varies between data points [30],
- (ii) using experimentally estimated values of the parameter β , which varies between data points,
- (iii) improved modelling of fluctuations of the fraction of protons for a given number of accepted baryons,
- (iv) taking into account the production of nuclear clusters,
- (v) taking into account the nuclear critical point which can significantly enhance the baryon number fluctuations at low collision energies [31].
- (vi) studying the sensitivity of the predictions to the QGP equation of state,
- (vii) investigating the sensitivity of the results to the assumption that net-baryon fluctuations freeze out in the vicinity of the chemical freeze-out line.

The results presented here open the possibility for a consistent interpre-

tation of experimental data from GSI SIS through CERN SPS to BNL RHIC and the CERN LHC.

Acknowledgements

The authors thank Stanislaw Mrowczynski, Volker Koch, and Volodymyr Vovchenko for reading the manuscript and providing fruitful comments.. This work was supported by the Polish National Science Centre (NCN) grant 2018/30/A/ST2/00226 and the National Research Foundation of Ukraine under grant 2025.07/0050.

Appendix A. The binomial thinning

It is assumed that for a fixed number of baryons, the proton number fluctuates according to a binomial distribution with the probability β – the so-called binomial thinning. Under the binomial thinning, the cumulants are modified according to the relations:

$$\frac{\kappa_2[p_A]}{\kappa_1[p_A]} = 1 - \beta + \beta \frac{\kappa_2[B_A]}{\kappa_1[B_A]}, \quad (\text{A.1})$$

$$\frac{\kappa_3[p_A]}{\kappa_2[p_A]} = \frac{\kappa_2[B_A]/\kappa_1[B_A]}{\kappa_2[p_A]/\kappa_1[p_A]} \left[\beta^2 \frac{\kappa_3[B_A]}{\kappa_2[B_A]} + 3\beta(1 - \beta) \right] + \frac{1 - \beta}{\kappa_2[p_A]/\kappa_1[p_A]} (1 - 2\beta), \quad (\text{A.2})$$

$$\begin{aligned} \frac{\kappa_4[p_A]}{\kappa_2[p_A]} = & \frac{\kappa_2[B_A]/\kappa_1[B_A]}{\kappa_2[p_A]/\kappa_1[p_A]} \left[\beta^3 \frac{\kappa_4[B_A]}{\kappa_2[B_A]} \right. \\ & \left. + 6\beta^2(1 - \beta) \frac{\kappa_3[B_A]}{\kappa_2[B_A]} + \beta(1 - \beta)(7 - 11\beta) \right] \\ & + \frac{1 - \beta}{\kappa_2[p_A]/\kappa_1[p_A]} [1 - 6\beta(1 - \beta)]. \end{aligned} \quad (\text{A.3})$$

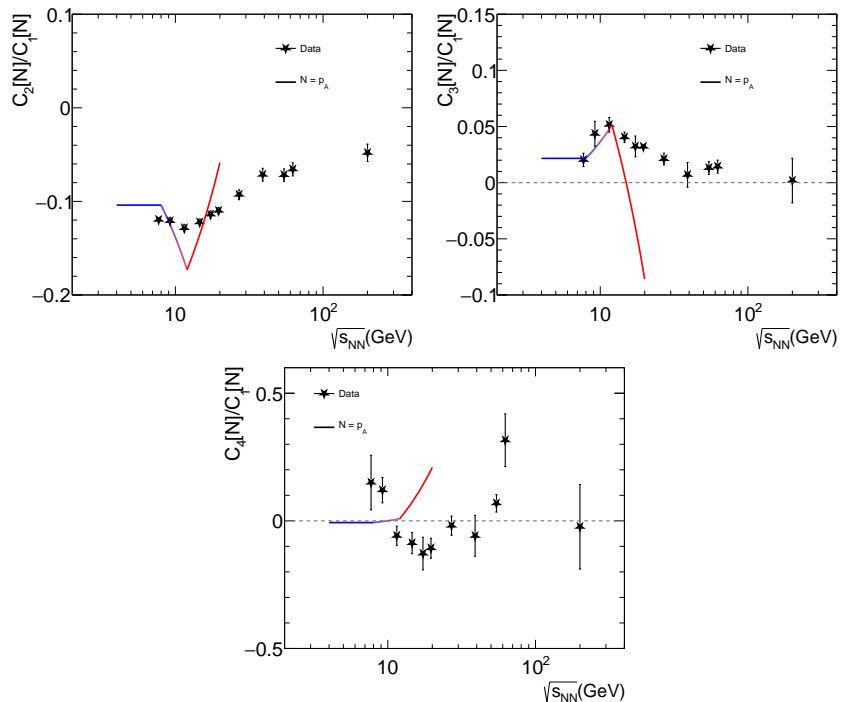


Figure B.4: Collision-energy dependence of the factorial cumulant ratios of the proton number in the acceptance. Symbols show measurements from the STAR experiment [32, 33], while solid lines correspond to our model calculations.

Appendix B. Comparison with experimental results

In this section, we compare the predictions of our model with the measured factorial cumulant ratios of the proton number reported by the STAR collaboration [9].

The relation between factorial cumulants C_n and ordinary cumulants κ_n is mediated by the signed Stirling numbers of the first kind $s(n, j)$

$$C_n = \sum_{j=1}^n s(n, j) \kappa_j, \quad (\text{B.1})$$

For the first four cumulants Eq. B.1 yields

$$C_1 = \kappa_1 \tag{B.2}$$

$$C_2 = -\kappa_1 + \kappa_2, \tag{B.3}$$

$$C_3 = 2\kappa_1 - 3\kappa_2 + \kappa_3,$$

$$C_4 = -6\kappa_1 + 11\kappa_2 - 6\kappa_3 + \kappa_4.$$

The considered cumulants ratios are

$$C_2/C_1 = -1 + \kappa_2/\kappa_1,$$

$$C_3/C_1 = 2 - 3\kappa_2/\kappa_1 + \kappa_3/\kappa_1, \tag{B.4}$$

$$C_4/C_1 = -6 + 11\kappa_2/\kappa_1 - 6\kappa_3/\kappa_1 + \kappa_4/\kappa_1.$$

Fig. B.4 shows the collision-energy dependence of the proton-number factorial cumulants measured by the STAR experiment [32, 33] (symbols) in comparison with our model calculations (solid lines). More specifically, our calculations for the equilibrium HRG are shown by blue lines for energies between 4 and 8 GeV. For energies above 12 GeV, the calculations correspond to the equilibrium QGP case. In general, the non-monotonic behaviour observed in the energy dependence of the measured cumulant ratios is qualitatively captured by the model predictions. For a more quantitative comparison, however, the remarks made in Section 4 need to be considered; these will be addressed in our future studies.

References

- [1] Edward V. Shuryak. Quantum Chromodynamics and the Theory of Superdense Matter. *Phys. Rept.*, 61:71–158, 1980.

- [2] S. V. Afanasiev et al. Energy dependence of pion and kaon production in central Pb + Pb collisions. Phys. Rev. C, 66:054902, 2002.
- [3] C. Alt et al. Pion and kaon production in central Pb + Pb collisions at 20-A and 30-A-GeV: Evidence for the onset of deconfinement. Phys. Rev. C, 77:024903, 2008.
- [4] Marek Gazdzicki and Mark I. Gorenstein. On the early stage of nucleus-nucleus collisions. Acta Phys. Polon. B, 30:2705, 1999.
- [5] L. Adamczyk et al. Bulk Properties of the Medium Produced in Relativistic Heavy-Ion Collisions from the Beam Energy Scan Program. Phys. Rev. C, 96(4):044904, 2017.
- [6] Anar Rustamov. The Horn, Kink and Step, Dale: from few GeV to few TeV. Central Eur. J. Phys., 10:1267–1270, 2012.
- [7] Marek Gazdzicki, Mark Gorenstein, and Peter Seyboth. Brief history of the search for critical structures in heavy-ion collisions. Acta Phys. Polon. B, 51:1033, 2020.
- [8] Adam Bzdak, Shinichi Esumi, Volker Koch, Jinfeng Liao, Mikhail Stephanov, and Nu Xu. Mapping the Phases of Quantum Chromodynamics with Beam Energy Scan. Phys. Rept., 853:1–87, 2020.
- [9] Mohamed Abdallah et al. Cumulants and correlation functions of net-proton, proton, and antiproton multiplicity distributions in Au+Au collisions at energies available at the BNL Relativistic Heavy Ion Collider. Phys. Rev. C, 104(2):024902, 2021. [Erratum: Phys.Rev.C 111, 029902 (2025)].

- [10] L. Adamczyk et al. Energy Dependence of Moments of Net-proton Multiplicity Distributions at RHIC. Phys. Rev. Lett., 112:032302, 2014.
- [11] J. Adamczewski-Musch et al. Proton-number fluctuations in $\sqrt{s_{NN}}=2.4$ GeV Au + Au collisions studied with the High-Acceptance DiElectron Spectrometer (HADES). Phys. Rev. C, 102(2):024914, 2020.
- [12] Shreyasi Acharya et al. Global baryon number conservation encoded in net-proton fluctuations measured in Pb–Pb collisions at sNN=2.76 TeV. Phys. Lett. B, 807:135564, 2020.
- [13] Shreyasi Acharya et al. Closing in on critical net-baryon fluctuations at LHC energies: Cumulants up to third order in Pb–Pb collisions. Phys. Lett. B, 844:137545, 2023.
- [14] M. A. Stephanov. Non-Gaussian fluctuations near the QCD critical point. Phys. Rev. Lett., 102:032301, 2009.
- [15] Bengt Friman, Krzysztof Redlich, and Anar Rustamov. Baselines for Abelian Charge Fluctuations in Nuclear Collisions: Theory and Comparison with Experimental Data. 8 2025.
- [16] Oleh Savchuk. Net-proton fluctuations influenced by baryon stopping and quark deconfinement. Phys. Rev. C, 111(2):024913, 2025.
- [17] Masayuki Asakawa, Ulrich W. Heinz, and Berndt Muller. Fluctuation probes of quark deconfinement. Phys. Rev. Lett., 85:2072–2075, 2000.
- [18] S. Jeon and V. Koch. Charged particle ratio fluctuation as a signal for QGP. Phys. Rev. Lett., 85:2076–2079, 2000.

- [19] Jacek Zaranek. Measures of charge fluctuations in nuclear collisions. Phys. Rev. C, 66:024905, 2002.
- [20] C. Alt et al. Electric charge fluctuations in central Pb+Pb collisions at 20-A-GeV, 30-A-GeV, 40-A-GeV, 80-A-GeV, and 158-A-GeV. Phys. Rev. C, 70:064903, 2004.
- [21] Betty Abelev et al. Net-Charge Fluctuations in Pb-Pb collisions at $\sqrt{s_{NN}} = 2.76$ TeV. Phys. Rev. Lett., 110(15):152301, 2013.
- [22] Jonathan Parra, Roman Poberezhniuk, Volker Koch, Claudia Ratti, and Volodymyr Vovchenko. Indications for Freeze-Out of Charge Fluctuations in the Quark-Gluon Plasma at the LHC. Phys. Rev. Lett., 135(24):242302, 2025.
- [23] M. Gazdzicki. The Mixed Phase Collision Energy Range from the Experimental Data. Acta Phys. Polon. B, 45(12):2319, 2014.
- [24] F. Becattini, J. Manninen, and M. Gazdzicki. Energy and system size dependence of chemical freeze-out in relativistic nuclear collisions. Phys. Rev. C, 73:044905, 2006.
- [25] J. I. Kapusta and Charles Gale. Finite-temperature field theory: Principles and applications. Cambridge Monographs on Mathematical Physics. Cambridge University Press, 2011.
- [26] Artemiy Lysenko, Mark I. Gorenstein, Roman Poberezhniuk, and Volodymyr Vovchenko. Chemical freeze-out curve in heavy-ion collisions and the QCD critical point. Phys. Rev. C, 111(5):054903, 2025.

- [27] J. Cleymans, H. Oeschler, K. Redlich, and S. Wheaton. Comparison of chemical freeze-out criteria in heavy-ion collisions. Phys. Rev. C, 73:034905, 2006.
- [28] Volodymyr Vovchenko, Oleh Savchuk, Roman V. Poberezhnyuk, Mark I. Gorenstein, and Volker Koch. Connecting fluctuation measurements in heavy-ion collisions with the grand-canonical susceptibilities. Phys. Lett. B, 811:135868, 2020.
- [29] Volodymyr A. Kuznietsov, Mark I. Gorenstein, Volker Koch, and Volodymyr Vovchenko. Coordinate versus momentum cuts and effects of collective flow on critical fluctuations. Phys. Rev. C, 110(1):015206, 2024.
- [30] P. Braun-Munzinger, B. Friman, K. Redlich, A. Rustamov, and J. Stachel. Relativistic nuclear collisions: Establishing a non-critical baseline for fluctuation measurements. Nucl. Phys. A, 1008:122141, 2021.
- [31] R. Poberezhnyuk, V. Vovchenko, A. Motornenko, M. I. Gorenstein, and H. Stoecker. Chemical freeze-out conditions and fluctuations of conserved charges in heavy-ion collisions within quantum van der Waals model. Phys. Rev. C, 100(5):054904, 2019.
- [32] B. E. Aboona et al. Precision Measurement of Net-Proton-Number Fluctuations in Au+Au Collisions at RHIC. Phys. Rev. Lett., 135(14):142301, 2025.

- [33] Peter Braun-Munzinger, Anar Rustamov, and Nu Xu. The phase structure of QCD: Fluctuations and Correlations. arXiv:2601.18666 [nucl-ex], 2026.